Desalination 279 (2011) 409–414

Contents lists available at ScienceDirect

Desalination

journal homepage: www.elsevier.com/locate/desal

Polysulfone/N-phthaloylchitosan novel composite membranes for salt rejection application

Mahesh Padaki [a], Arun M. Isloor [a,*], Pikul Wanichapichart [b,c,**]

[a] Membrane Technology Division, Chemistry Department, National Institute of Technology—Karnataka, Surathkal, Mangalore 575 025, India
[b] Membrane Science and Technology Research Center, Department of Physics, Prince of Songkla University, Hat Yai, Songkhla 90110, Thailand
[c] Thailand Center of Excellence in Physics, Commission on Higher Education, 328 Si Ayutthaya Road, Bangkok 10400, Thailand

ARTICLE INFO

Article history:
Received 4 March 2011
Received in revised form 20 June 2011
Accepted 21 June 2011
Available online 12 July 2011

Keywords:
N-phthaloylchitosan
Polysulfone
Water flux
PEG rejection
FT-IR analysis
Salt rejection

ABSTRACT

N-phthaloylchitosan (CS) was synthesized by the reaction of chitosan with phthalic anhydride in dimethyl formamide. Different compositions of polysulfone (PSf) and N-phthaloylchitosan were used to prepare novel polysulfone/N-phthaloylchitosan (PSf/CS) composite membranes by phase inversion method. The composition ratios between the former and the latter were 80:20, 85:15, 90:10, and 95:5. Water flux results revealed that, PSf:CS 80:20 membrane is found to have greatest effective pore area while PSf:CS 95:05 membrane has the smallest value. The pore area is found to be larger with the increase in CS composition. In addition, its water swelling property increases with the increase of CS composition. Water flux results are in consistent with dielectric constant value. Use of known molecular weight of polyethylene glycol rejection study, revealed that, PSf:CS 95:05 membrane possessed the smallest pore size among these membranes. In conclusion, change of ratio between PSf and CS, considerably affects membrane pore size and hydrophilicity. For salt filtration, membrane PSf:CS 95:05 showed 93%, 76.11% and 70.12% rejection of $MgSO_4$, Na_2SO_4, and NaCl, respectively.

1. Introduction

Conventional desalination and water purification using membrane technology have grabbed researchers' interest for many years. Separation at solid/liquid interface can be carried out continuously under mild conditions with low energy consumption [1]. Membrane properties are variable and pore size can be adjustable according to their applications [2]. Membrane technology is widely applicable in many areas such as, chemical and biochemical processes, stream separation, sea water desalination, removal of heavy metals from waste effluents, and purification of potable water [3–7]. With the emerging research in nanotechnology, nanofiltration membranes play important role in nano-safety, to remove toxic nano-particles (<100 nm) from the environment.

Transport mechanism of porous membrane is not yet completely understood. Several models have been proposed to explain the transport mechanism of the porous membrane using Teorell–Meyer–Sievers model (TMS) [8], the space-charge model [9], and the extended Nernst–Plank equation [10]. Continuation by Nernst–Plank equation coupled with Donnan equilibrium has been used to describe the separation performance of amphoteric pores membrane based on convection, diffusion, and electromigration [11,12]. However, current work [13,14] reveals that dielectric effects are also not to be neglected in the complex separation mechanisms.

Polysaccharides, as in chitosan, are hydrophilic in nature having many hydroxyl groups and generally have relatively good biocompatibility. It contains primary amino groups obtained by N-deacetylation of a natural polymer chitin and noteworthy as non-toxic, biocompatible and non-immunogenetic polysaccharide [15,16]. Therefore chitosan has wide variety of the applications. Also, highly reactive primary amino groups of the chitosan are convenient for chemical modification, having better solubility in organic solvent so it is easier to compose with other polymer to get a homogenous membrane. Zheng et al. [17] reported the synthesis of N,O-carboxymethyl chitosan (NOCC) and cellulose acetate blend film. The NOCC, a water-soluble chitosan derivative, is a carboxylated chitosan having carboxymethyl substituents on some of the both amino and primary hydroxyl sites of the glucosamine units of the chitosan structure [18]. In addition, it is hydrophilic and a typical kind of amphoteric polyelectrolyte with anticancer and antibacterial [19] property. At the same time, it is found to be a potential candidate for microfiltration [20] and pervaporation [21] by appropriate modification.

Ohya et al. [16] reported graft styrene polymerisation of chitosan, where N-phthaloylchitosan was employed for chemical modification. Its 6-O-trityl protection of chitosan through N-phthaloylchitosan [22,23] is another effective method to achieve homogenous chitosan

* Correspondence to: A.M. Isloor, Membrane Technology Division, Chemistry Department, National Institute of Technology-Karnataka, Surathkal, India. Fax: +91 824 2474033.
** Correspondence to: P. Wanichapichart, Membrane Science and Technology Research Center, Department of Physics, Prince of Songkla University, Hat Yai, Songkhla 90110, Thailand. Fax: +66 74288754.
E-mail addresses: isloor@yahoo.com (A.M. Isloor), pikul.v@psu.ac.th (P. Wanichapichart).

0011-9164/$ – see front matter © 2011 Elsevier B.V. All rights reserved.
doi:10.1016/j.desal.2011.06.045

modification at the amino group with good yield. N-phthaloylchitosan is soluble not only in a weak acid, but also in some organic solvents, so it is very useful to prepare the composite membranes with polysulfone. However, to our knowledge until now, there is no any proper literature on composite porous membranes using N-phthaloylchitosan.

In this work, N-phthaloylchitosan was synthesized by reacting chitosan with phthalic anhydride in dimethylformamide. The mixture of polysulfone and N-phthaloylchitosan in different compositions was used to prepare polysulfone/N-phthaloylchitosan (PSf/CS) novel composite membranes. Further they were verified by means of water flux study, dielectric constant, and filtration using mono- and divalent salt solutions. Rejection of polyethylene glycol (PEG) was also investigated to estimate types of these novel filtration membranes.

2. Materials and methods

2.1. Materials

Chitosan (MW 5.4×105, 91% degree of deacetylation) and polysulfone (PS) (MW 35000 Da) were purchased from Seafresh Company Ltd., Thailand and Sigma Aldrich, respectively. Phthalic anhydride and NMP (N-methylpyrrolidone) were of analytical grade and used without further purification. The G4 sand filters were purchased from local market of Hat-Yai, Thailand for the filtration of casting solution. Deionised water was used for membrane preparation and permeation experiments. Salt solutions of NaCl, Na_2SO_4 and $MgSO_4$ were used for feed and permeate was determined using conductivity meter. The IR spectra were recorded on an Avatar 360 IR spectrophotometer.

2.2. Preparation of the N-phthaloylchitosan

Chitosan modification was done according to the procedure reported by Yoksam and Chirachanchai [24]. In brief, 23.7 g chitosan (MW 5.4×10^5, 91% degree of deacetylation) was reacted with 64.5 g phthalic-anhydride in 100 mL DMF (dimethylformamide) at 130 °C for 5 h, under nitrogen atmosphere. The reaction mixture was poured into a large amount of ice-cold water to precipitate N-phthaloylchitosan. It was, then filtered and purified by ethanol and ethyl ether to obtain yellow solid with 80.6% yield. The FT-IR spectra of N-phthaloylchitosan was recorded using KBr pellets in the range of 4000–400 cm^{-1} to confirm the structure. The synthetic route for the same has been presented in Fig. 1.

2.3. Preparation of composite membranes

Membranes were prepared by phase inversion method [25]. Polysulfone (Sigma Aldrich, 35000 Da) and the prepared N-phthaloylchitosan, of different ratio were dissolved in NMP (N-methylpyrrolidone) at 60 °C for 24 h to get clear solution. The so obtained viscous solution was filtered by G4 sand filter before casting. The membrane was prepared by casting viscous solution on a glass plate. The thickness of the wet membrane was maintained at 0.2 mm. It was, then, evaporated at 25±1 °C for 30 seconds, and immersed in a coagulation water bath for 30 min. In the coagulation bath containing distilled water, demixing of solvent takes place. Hence it necessary to change the distilled water. Finally the membrane was washed and stored in distilled water for further characterization.

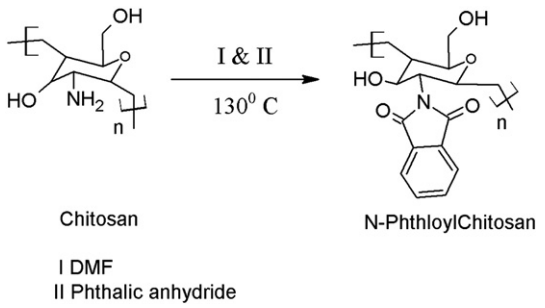

Fig. 1. Schematic representation of the synthesis of N-phthaloylchitosan.

2.4. Membrane characterization

ATR-IR of the membrane was recorded using Avatar 360 IR spectrophotometer in the range of 4000–400 cm^{-1}.

Hydrophilicity of the membrane was determined by swelling behavior and contact angle measurement. The former was studied by weight change during swelling in distilled water. The several pieces of membranes having 1 cm^2 area were thoroughly rinsed with distilled water, and then dried in desiccator for 24 h. These dried membranes were later immersed in distilled water for at least 24 h. The swollen membranes were taken out at a series of time, and excess water on the surface was gently removed by a blotter. Then the swollen weights of membranes were quickly measured. Later, membranes were again dried under vacuum desiccator for 24 h and weighed. Degree of swelling was calculated using the equation

$$\%\text{swelling} = \left(\frac{W_w - W_d}{W_d}\right) \times 100,$$

where W_w and W_d are the weight of wet and dried membranes, respectively.

Contact angle of the membrane surface was measured with a measurement apparatus (OCA 15 EC, Germany). The measurement was done according to the sessile droplet method. In brief, a water droplet was deposited on a flat homogenous membrane surface and the contact angle of the droplet with surface was measured. The value was observed until there was no change in contact angle during short measurement period. Each contact angle was measured three times at different points of each membrane sample and an average value was calculated using standard deviation curve.

Dielectric constant of the membrane was determined by using Precision LRC meter Agilent 4258A with 16451b dielectric test fixture at various frequencies 75 kHz to 30 MHz with 1 MHz steps.

2.5. Permeation experiments

2.5.1. Hydraulic permeability coefficient of the membrane

Water flux study has been done by using dead end flow cell. The effective area of the membrane was 50 mM. Hydraulic permeability of the membrane (L_p) was estimated from slope between water flux and the applied pressure $L_p = \text{slope} \times 2.77 \times 10^{-10}$.

2.5.2. Rejection study of membranes

The rejection experiment was carried out as same as water flux study. PEG of several molecular weights (6000–10000 Da) at 50 ppm was filtered in a dead end unit and permeate was estimated using spectrophotometer [26]. 4 mL of permeate sample solution was added to 1 mL of reagent A (5% (w/v) $BaCl_2$ in 1N HCl) and reagent B (1.27 g I_2 in 100 mL 2% KI (w/v) solution). This mixture was allowed to develop the color for 15 min at room temperature and absorption was measured using a spectrophotometer at 535 nm against a blank reagent.

Feed of 1000 ppm of Na_2SO_4, NaCl and $MgSO_4$ solutions was used as inorganic electrolytes. Salt concentration was filtered with the composite membranes, and the content in feed and permeate was measured using a conductivity meter. Rejection of both PEG and salt was calculated with

$$\%R = \left(1 - \frac{C_p}{C_f}\right) \times 100$$

where C_p and C_f represent the concentrations of permeate (p) and feed (f), respectively. The presented data are the average of three measurements conducted on two pieces of membranes cut from a single sheet.

3. Results and discussion

FT-IR spectra of the N-phthaloylchitosan were measured for confirmation of the product by KBr pellet method [8]. Fig. 2, shows the peaks at 3447 cm^{-1} of the OH group, 2922 cm^{-1} of the C—H group, 1703 cm^{-1} of the imide C O, 1381 cm^{-1} C—N group, 1058 cm^{-1} of the C—OH group and 714 cm^{-1} of the aromatic C C group. Fig. 2b represents the ATR-IR spectra of the membranes. The characteristic peaks of the N-phthaloylchitosan at 3345 cm^{-1}–3361 cm^{-1} of the OH group, 2965 cm^{-1}–2968 cm^{-1} of the C—H group and C O peak shifted to the lower side of 1664 cm^{-1}–1679 cm^{-1}. C—N and C—OH groups shifted to the 1013 cm^{-1} to

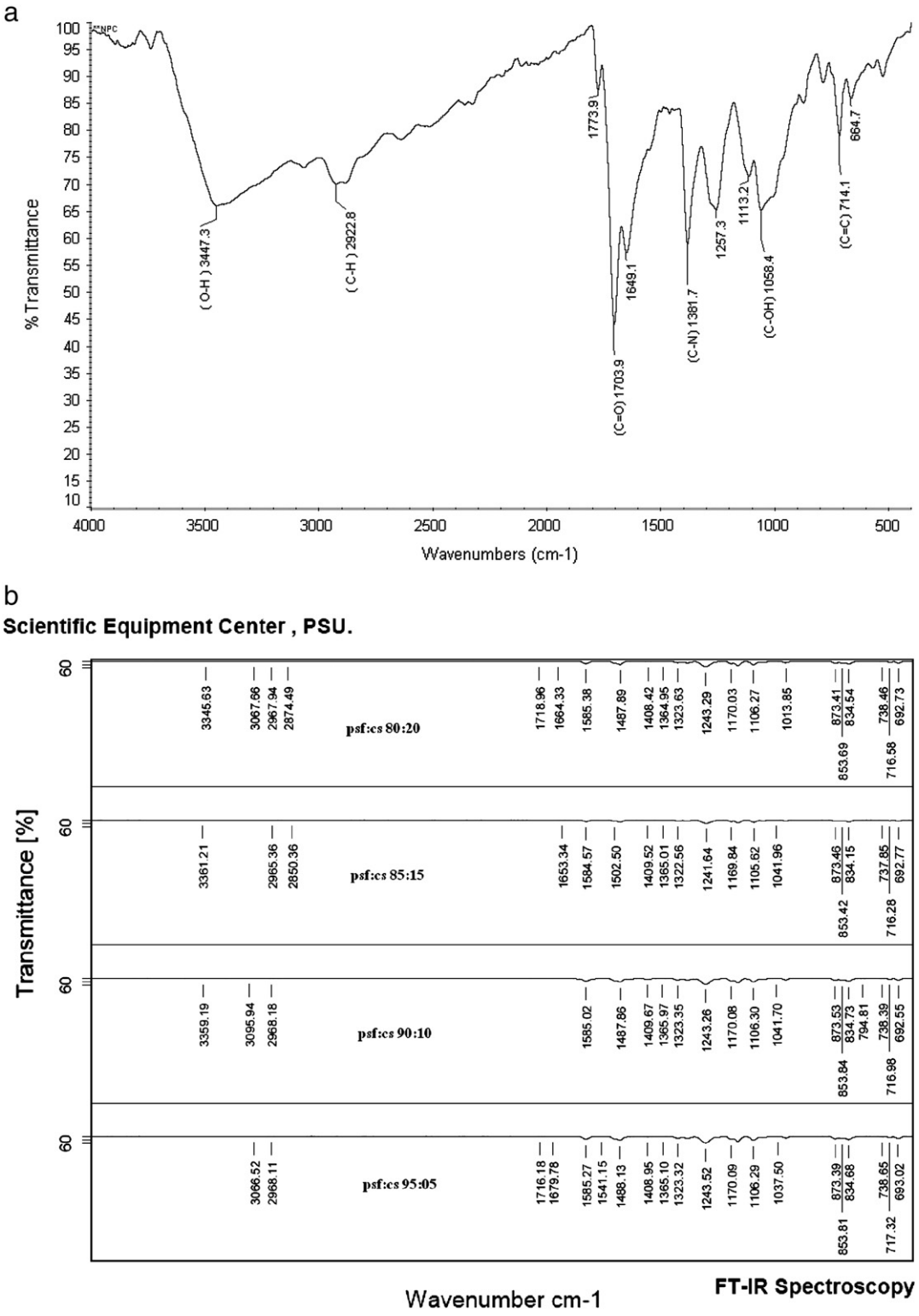

Fig. 2. a. FT-IR spectrum of the N-phthaloylchitosan. b. ATR-IR spectrum of the membranes.

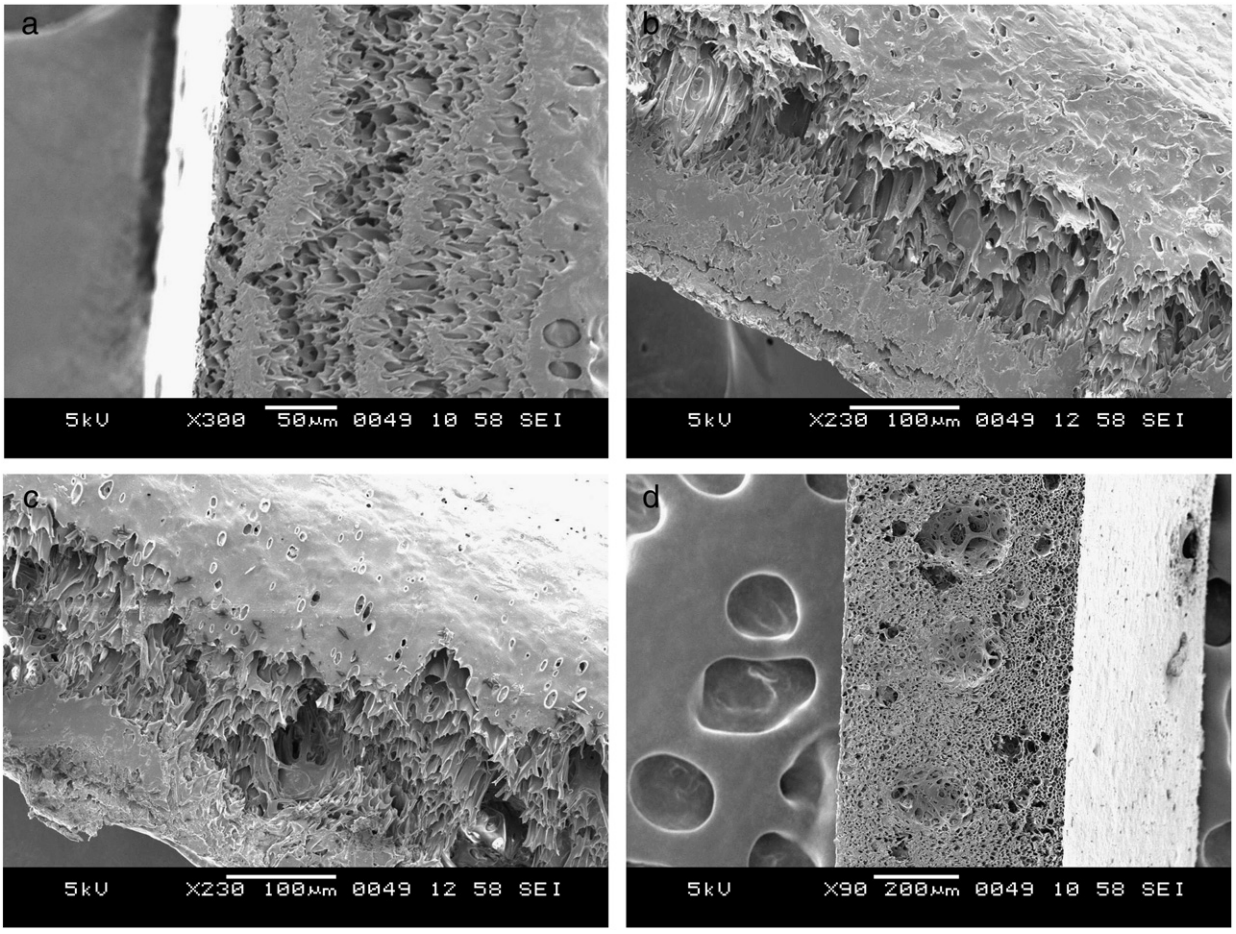

Fig. 3. a. Cross section image of PSf:CS 80:20. b. Cross section image of PSf:CS 85:15. c. Cross section image of PSf:CS 90:10. d. Cross section image of PSf:CS 95:05.

1041 cm^{-1} and 737 cm^{-1} to 738 cm^{-1} respectively. The presence of strong peak at 1241 cm^{-1} to 1243 cm^{-1} is assigned to the ether C—O—C stretch of the polysulfone moiety and the peak at 1169 cm^{-1} to 1170 cm^{-1} due to O S O stretching.

Membranes could not withstand high temperature and hence it was not possible to prepare SEM micrograph of surface. Cross section images were taken in lower magnification. Fig. 3a to d represents the cross section images of the membranes. Increase of CS concentration results in diminishing of finger-like structure, however formation of thick sponge like structures. It can be explained by phase separation process. In this case the increase of CS concentration decreases the exchange between inner casting solution and water, and thereby weaker stress derived from the shrinkage of polymer-rich phase. Hence, phase separation was limited. Therefore, there is decrease in finger-like pores and the sponge-like structure was more dominant.

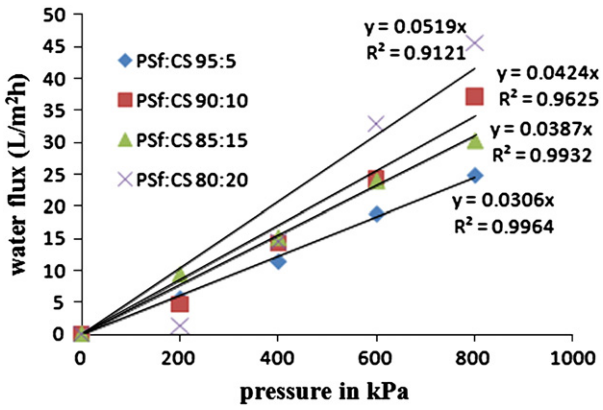

Fig. 4. Water flux of the composite membranes.

Pure water permeability was obtained by measuring the flux for pure water against operating pressure. As shown in Fig. 4, the flux increases linearly with the operating pressure. The composition of the PSf:CS 95:5 shows the lowest flux and PSf:CS 80:20 shows the highest flux. This relation is close to pure water permeability according to the Spiegler–Kedem model [27]. The hydraulic permeability coefficient of the membrane has been shown in Table 1. The increasing CS composition in the membrane increases the water flux and, hence, hydraulic permeability coefficient.

Fig. 5 represents the dielectric spectrum, which is independent of the frequencies between 4×10^6 and 7×10^6 Hz. Among the four compositions, the membrane PSf:CS 80:20 possesses the smallest dielectric constant. Both membrane PSf:CS 95:05 and PSf:CS 90:10 possess the same dielectric values and being the maximum value. As discussed in Ref. [28], the maximum dielectric constant represented the smallest void area of the membrane, and this was verified by the minimum water flux shown in Fig. 4.

Fig. 6 shows the water swelling study under different pH. pH variation was done by using conc. HCl and 4% NaOH solution.

Table 1
Contact angle and hydraulic permeability coefficient of the membranes.

Membrane	Contact angle	L_p in (m/sPa)
PSf:CS 95:05	89±2	8.48×10^{-12}
PSf:CS 90:10	86±2	0.11×10^{-12}
PSf:CS 85:15	75±2	0.12×10^{-12}
PSf:CS 80:20	73±2	0.14×10^{-12}

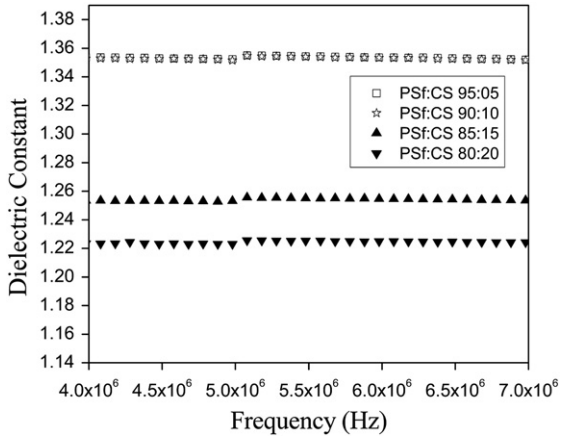

Fig. 5. Dielectric constant of the membranes.

The membrane PSf:CS 80:20 shows the greatest water swelling than the other for all pH used. It is interesting to observe that, all membranes perform similar pattern changes in the swelling percentage. The greater swelling percentage is related to the greater CS content. As a consequence, contact angle was studied and the results are shown in Table 1. As expected, the membrane PSf:CS 80:20 showed the smallest contact angle while the opposite is the case for the PSf:CS 95:05 one, since PSf is hydrophobic material and the addition of CS reduced the property, and resulted in decrease of the contact angle. In the pH range of 4–5, membranes showed the highest water swelling. This is due to the amide bond in N-phthaloylchitosan, which readily undergoes protonation and leads to higher water swelling whereas, in higher pH 3, the unstable amide bond breaks and resulted in low water swelling. In neutral and basic pH, there is no sign of protonation and hence, the water swelling decreases.

The prepared membrane was further investigated by filtering known molecular weight PEG solution. Fig. 7 represents rejection of PEG according to the MW used. The membrane PSf:CS 95:05 showed PEG (6000 Da) rejection of 80%, while for PEG (10000 Da), it was found to be nearly 90% rejection. The remaining membranes possess larger pore size and hence exhibit less PEG rejection in order with the CS content. Hence the membrane PSf:CS 95:05 is nanofiltration membrane and the remaining are ultrafiltration membranes.

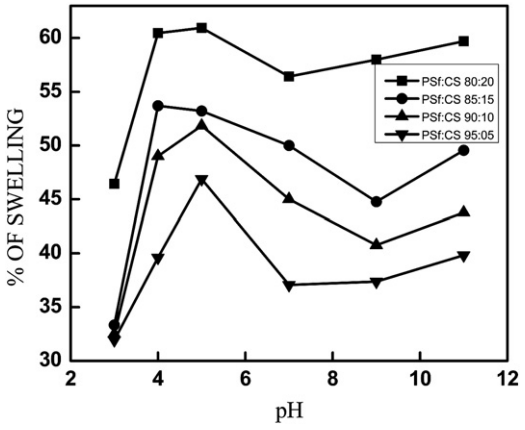

Fig. 6. Effect of pH on water swelling property.

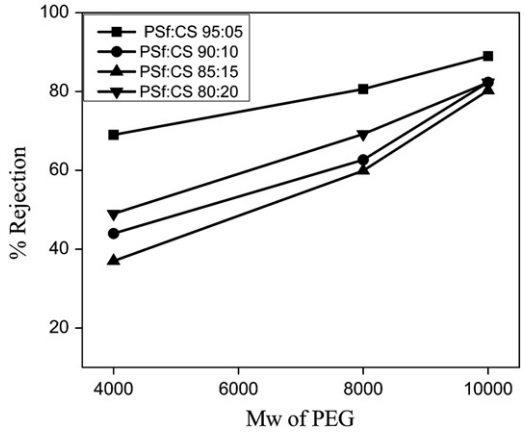

Fig. 7. PEG rejection of the membranes.

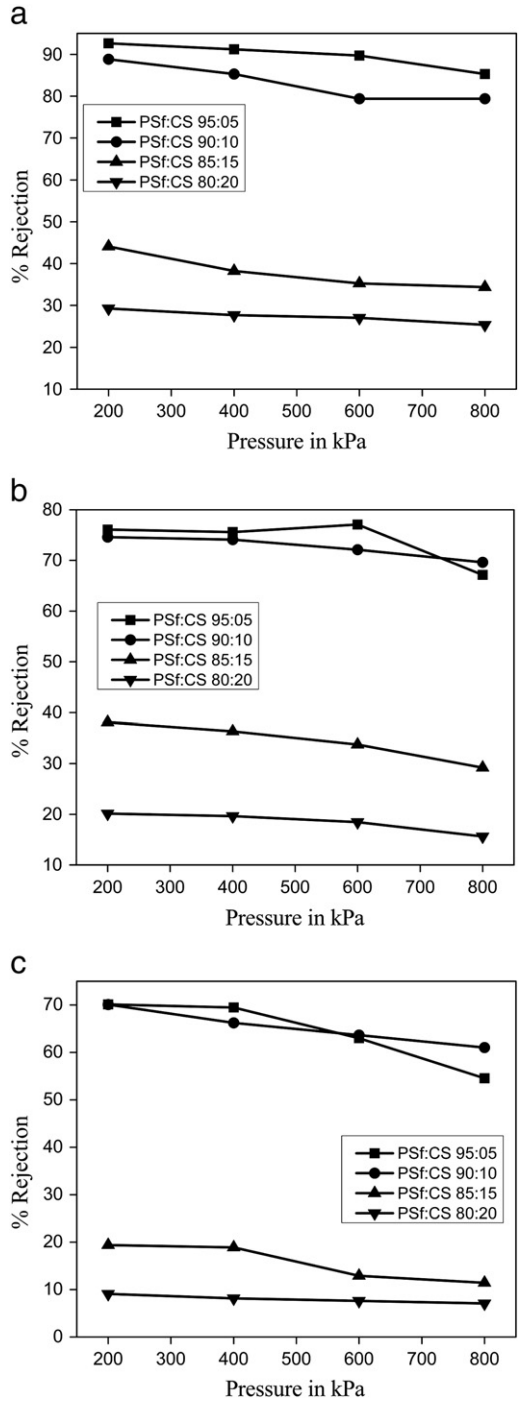

Fig. 8. (a) $MgSO_4$ rejection. (b) Na_2SO_4 rejection. (c) NaCl rejection.

Salt rejection of the membranes is presented in Fig. 8(a–c). It is interesting to observe that, there is a tendency of a decline in salt rejection under higher applied pressures in all cases. It might be due to some convection flow, leading to an increase in permeate salt concentration. While comparing among electrolyte used, the rejection of electrolyte solution decreases in the following order $MgSO_4$, Na_2SO_4 and NaCl as shown in Fig. 8(a–c). Higher rejection of $MgSO_4$ over NaCl can be explained using size exclusion principle, as SO_4^- is larger in size than that of Cl^-, so it showed greater rejection. The membrane PSf:CS 95:05 showed the greatest rejection for $MgSO_4$ at about 93%, and that for Na_2SO_4 and NaCl are 76.11% and 70.12%, respectively. The PSf:CS 80:20 shows the smallest rejection for $MgSO_4$, Na_2SO_4, and NaCl at about 28.5%, 22.5% and 13.6%, respectively. These results confirmed that the membrane PSf:CS 95:05 possessed the smallest pore size, compared to the others. In addition, it implies that, the smallest effective pore area in Figs. 4 and 5 directly indicates the smallest pore size and also MWCO study, in that PSf:CS 95:05 shows the lowest MWCO as compared to other membranes.

It is interesting to point out that greater $MgSO_4$ rejection in membrane PSf:CS 95:05 than membrane PSf:CS 90:10 indicated that the former has smaller pore size than the latter, whereas the comparative pore size between these two membranes could not be distinguished if NaCl was used for testing.

4. Conclusions

FT-IR analysis confirmed the formation of N-phthaloylchitosan. Composite membranes performed a range of nano- to ultra-filtration according to the CS content. The increase in CS content induced membrane hydrophilicity, leading to water swelling and membrane pore size enlargement. In addition, the membrane swelling property is pH dependent. The smallest swelling occurred at pH 3 and was maximized to 65% at pH 5–6. Membrane PSf:CS 95:05 and 90:10 performed nano-filtration with 95% of $MgSO_4$ rejection, 78% of Na_2SO_4 rejection and 75% of NaCl rejection, respectively. The PSf:CS 85:15 and 80:20 were classified as ultra-filtration membranes with much smaller rejection for the above salts.

Acknowledgments

We sincerely acknowledge National Institute of Technology—Karnataka India and the Membrane Science and Technology Research Center of Prince Songkla University, Thailand for supporting this collaborative research. Thanks are also due to Assoc. Prof. Suchada Chantraprooma, Chemistry Department of Prince of Songkhla University, Hat Yai, Thailand for extending the support to carry out chemical synthesis. A.M.I. thanks Department of Atomic Energy, Board for Research in Nuclear Sciences, Government of India for "Young Scientist" award.

References

[1] E. Drioli, L. Giorno, Membrane operations, Wiley-VCH Verlag Gmbh & Co. KGaA, 2009.
[2] N.C. van de Merbel, J.J. Hageman, U.A.Th. Brinkman, Membrane-based sample preparation for chromatography, J. Chromatogr. 634 (1993) 1–29.
[3] K. TreVry-Goatley, C. Buckley, G. Groves, Reverse osmosis treatment and reuse of textile dyehouse effluents, Desalination 47 (1983) 313–320.
[4] M.E. Williams, D. Bhattacharyya, R.J. Ray, S.B. McCray, Reverse osmosis: selected applications, in: W.S.W. Ho, K.K. Sirkar (Eds.), Membrane Handbook, Van Nostrand Reinhold, New York, 1992.
[5] H.C. van der Host, J.M.K. Timmer, T. Robbertsen, J. Lenders, Use of nanofiltration for concentration and demineralization in dairy industry: model for mass transport, J. Membr. Sci. 104 (1995) 205–218.
[6] J.M.K. Timer, H.C. van-der Horst, T. Robbertsen, Transport of lactic acid through reverse osmosis and nanofiltration membranes, J. Membr. Sci. 85 (2) (1993) 205–216.
[7] J.M.K. Timer, J. Kromkamp, T. Robbertsen, Lactic acid separation from fermentation broths by reverse osmosis and nanofiltration, J. Membr. Sci. 92 (1994) 185–197.
[8] E. Hoffer, O. Kedem, Hyperfiltration in charged membranes: the fixed charged model, Desalination 2 (1967) 25–39.
[9] R.J. Gross, J.F. Osterle, Membrane transport characteristic of ultrafine capillaries, J. Chem. Phys. 49 (1) (1968) 228–234.
[10] S.R. Stoff, Transport Durch Membrane, Darmstadt, , 1964.
[11] P. Fievet, C. Labbez, A. Szymczyk, et al., Electrolyte transport through amphoteric nanofiltration membranes, Chem. Eng. Sci. 57 (2002) 2921–2931.
[12] M.D. Afonso, M.N. de Pinho, Transport of MgSO4, MgCl2, and Na2SO4 across an amphoteric nanofiltration membrane, J. Membr. Sci. 179 (2000) 137–154.
[13] A.E. Yaroshchuk, Dielectric exclusion of ions from membranes, Adv. Colloid Interface Sci. 85 (2000) 193–230.
[14] A. Szymczyk, P. Fievet, Investigating transport properties of nanofiltration membranes bymeans of a steric, electric and dielectric exclusion model, J. Membr. Sci. 252 (2005) 77–88.
[15] S. Harino, H. Saino, Y. Akiyama, I. Nonaka, Progress in Biomedical Polymers, Plenum Press, New York, 1990.
[16] Y. Ohya, S. Marushashi, K. Shizuno, S. Mano, J. Murata, T. Ouchi, Graft polymerization of styrene on chitosan and the characteristics of the polymer, J. Macromol Sci. Part-A 36 (1999) 339–353.
[17] E.R. Hayes, N, O-carboxymethyl chitosan and preparative method, US Patent 4619995 (1986).
[18] K.X. Wu, M.N. Li, The immune regulation of carboxymethyl polysaccharides, Chin. Chem. Bull. 9 (1999) 54–57.
[19] H. Zheng, Y.M. Du, Structure and antibacterial activity of cellulose carboxymethylation chitosan blend films, Polym. Mater. Sci. Eng. (Chin.) 18 (4) (2002) 124–127.
[20] Z.P. Zhao, Z. Wang, S.C. Wang, Formation, charged characteristic and BSA adsorption behavior of carboxymethyl chitosan/PES composite MF membrane, J. Membr. Sci. 217 (2003) 151–158.
[21] Y.M. Lee, Modified chitosan membranes for pervaporation, Desalination 90 (1993) 277–290.
[22] S. Nishimura, O. Khonga, K. Kurita, C. Vittavatvong, H. KuZuhara, Chem. Lett. 19 (1990) 243–246.
[23] S. Nishimura, O. Khonga, K. Kurita, C. Vittavatvong, H. KuZuhara, Macromolecules 24 (1991) 4745–4748.
[24] R. Yoksam, S. Chirachanchai, Amphiphilic chitosan nanosphere: studies on formation, toxicity, and guest molecule incorporation, Biorganics & Medicinal Chemistry 16 (2008) 2687–2696.
[25] C. Hegde, A.M. Isloor, M. Padaki, P. Wanichapichart, Y. Liangdeng, Synthesis and desalination performance of Ar+−N+ irradiated polysulfone based new NF membrane, Desalination 265 (2011) 153–158.
[26] A.D. Sabde, M.K. Trivedi, V. Ramachandhran, M.S. Hanra, B.M. Misra, Casting and characterization of cellulose acetate butyrate based UF membranes, Desalination 114 (1997) 223–232.
[27] Y.Z. Xu, R.E. Lebrun, Comparison of nanofiltration properties of two membranes using electrolyte and nonelectrolyte, Desalination 122 (1999) 95–106.
[28] B. Jaleh, P. Parvin, P. Wanichapichart, A. Pourakbar Saffar, A. Reyhani, Induced super hydrophilicity due to surface modification of polypropylene membrane treated by O_2 plasma, Appl. Surf. Sci. 257 (2010) 1655–1659.